J. Phys. B: At. Mol. Phys. **18** (1985) 1637-1660. Printed in Great Britain

Elastic and inelastic scattering of electrons and positrons by atomic hydrogen at intermediate and high energies in the unitarised eikonal-Born series method

F W Byron Jr†, C J Joachain‡§ and R M Potvliege‡

† Department of Physics and Astronomy, University of Massachusetts, Amherst, Massachusetts 01003, USA

‡ Physique Théorique, Faculté des Sciences, Université Libre de Bruxelles, Brussels, Belgium

§ Institut de Physique Corpusculaire, Université de Louvain, Louvain-la-Neuve, Belgium

Received 7 November 1984

Abstract. The eikonal-Born series approximation is unitarised by using an improved Wallace-type amplitude to construct the direct scattering amplitude. The new unitarised eikonal-Born series (UEBS) direct amplitude obtained in this way is first tested successfully in potential scattering. It is then generalised to electron- and positron-atom collisions, and applied to elastic (1s-1s), 1s-2s and 1s-2p transitions in atomic hydrogen. The large momentum transfer properties of our UEBS direct amplitude are analysed for these three transitions, and the structure of the third term of the Born series is investigated by using the unitarity relations. Exchange effects are also discussed. Our theoretical results are compared with those obtained from other theories and with recent measurements, for impact energies ranging from 54.4 to 400 eV.

1. Introduction

The scattering of electrons by ground-state hydrogen atoms is a problem of fundamental interest in atomic collision theory. At low electron impact energies, where only a finite number of channels are open, theoretical methods based on the close-coupling approximation, improved by the inclusion of pseudostates and correlation functions (see for example Burke and Williams 1977) have been very satisfactory. At high energies (say above 200 eV), perturbative methods such as the eikonal-Born series theory (see for example Byron and Joachain 1977) or the distorted-wave second Born approximation (Kingston and Walters 1980) have also been very successful, at least in describing direct collisions, which are dominant at these energies. In contrast, in the intermediate energy range (extending from the ionisation threshold to about 200 eV) very complicated theoretical problems arise, the basic difficulty being to allow for the infinite number of open channels (including continuum ones) in a region where the use of the first few terms of the perturbation series is often insufficient, particularly for large scattering angles. Thus, even the simplest transitions which we shall consider in this article, namely elastic scattering and excitation of the 2s and 2p states, constitute at intermediate energies a very serious challenge to the theorist. These transitions have been the subject of a number of elaborate calculations during recent years (see for example Kingston *et al* 1976, 1982, Kingston and Walters 1980, Fon *et al* 1981, Byron and Joachain 1981, Byron *et al* 1981, 1982, Bransden *et al* 1982, Edmunds *et al* 1983, McCarthy and Stelbovics 1983a, b, c, Madison 1984).

In this paper we present the results of our theoretical investigations of this problem, performed within the framework of the unitarised eikonal-Born series (UEBS) method which we proposed recently (Byron *et al* 1981, 1982). This method is based on the many-body generalisation of an improved eikonal scattering amplitude derived by Wallace (1973), suitably modified to eliminate the difficulties arising in second order in the projectile-target interaction due to the zero-excitation-energy approximation involved in the many-body Wallace amplitude. The resulting direct UEBS amplitude is an all-order, nearly unitary scattering amplitude which retains all the advantages of the EBS direct amplitude at small and intermediate angles, but is more accurate at large angles. A non-perturbative approximation scheme for the exchange amplitude has also been developed (Byron *et al* 1982) which is appropriate to use in conjunction with the direct UEBS amplitude.

The organisation of this paper is as follows. We begin in § 2 by presenting new results we have obtained in potential scattering concerning improved eikonal expansions for the scattering amplitude. These results are used to construct an improved many-body Wallace amplitude and hence the corresponding UEBS direct amplitude. We then analyse the large momentum transfer properties of the direct amplitude for the three transitions considered (1s-1s, 1s-2s, 1s-2p) and make a detailed study of third-order effects. We conclude § 2 by a discussion of exchange effects. Section 3 is devoted to the presentation and discussion of our results, for electron impact energies ranging from 54.4 to 400 eV; these results are compared with other recent calculations and with the experimental data. We also present in § 3 new results we have obtained for elastic and total positron-atomic-hydrogen cross sections. Atomic units will be used throughout this paper, and the notation is that introduced in Byron *et al* (1982), to be referred to as I.

2. Theory

2.1. Potential scattering

Let us consider the scattering of an electron or a positron by a static potential $V(\boldsymbol{r})$. We denote by $\bar{f}_{\mathrm{B}n}$ the term of order n of the Born series, by f_{E} the eikonal (Glauber) scattering amplitude (see equation (2.1) of I) and by $\bar{f}_{\mathrm{E}n}$ the term of order n in the eikonal series (obtained by expanding the amplitude f_{E} in powers of the interaction potential). The starting point of the UEBS method discussed in our previous work was the potential scattering Wallace amplitude (Wallace 1973) as given by equation (2.7) of I. That is,

$$f_{\mathrm{W}}=\frac{k}{2\pi\mathrm{i}}\int \mathrm{d}^2\boldsymbol{b}\,\exp(\mathrm{i}\boldsymbol{\Delta}\cdot\boldsymbol{b})\{\exp[\mathrm{i}(k^{-1}\chi_0(\boldsymbol{b})+k^{-3}\chi_1(\boldsymbol{b}))]-1\} \tag{2.1}$$

where $\boldsymbol{\Delta}=\boldsymbol{k}_i-\boldsymbol{k}_f$ is the momentum transfer, $k=|\boldsymbol{k}_i|=|\boldsymbol{k}_f|$, $\chi_0(\boldsymbol{b})$ is the eikonal phase (see equation (2.2) of I) and $\chi_1(\boldsymbol{b})$ is the leading Wallace phase correction (see equations (2.8)-(2.10) of I) which is of second order in the interaction potential. We recall that we are working in a cylindrical coordinate system, with $\boldsymbol{r}=\boldsymbol{b}+z\hat{\boldsymbol{n}}$, $\hat{\boldsymbol{n}}$ being the direction perpendicular to $\boldsymbol{\Delta}$ in the scattering plane. The Wallace series is defined by expanding the amplitude f_{W} in powers of the potential. Calling $\bar{f}_{\mathrm{W}n}$ the term of order n in the potential strength, we have $\bar{f}_{W1}=\bar{f}_{E1}=\bar{f}_{B1}$ (see equation (2.12) of I) while for $n\geqslant 2$

$$\bar{f}_{Wn}=\left(\frac{i}{k}\right)^{n-1}\frac{1}{2\pi n!}\int d^2\boldsymbol{b}\exp(i\boldsymbol{\Delta}\cdot\boldsymbol{b})\left(\chi_0^n(\boldsymbol{b})-n(n-1)\frac{i}{k}\chi_0^{n-2}(\boldsymbol{b})\chi_1(\boldsymbol{b})+\dots\right) \tag{2.2}$$

so that

$$\bar{f}_{Wn}=\bar{f}_{En}[1+O(k^{-1})] \qquad n\geqslant 2. \tag{2.3}$$

Additional phase corrections (Wallace 1973) must be included in equation (2.2) if one wants to correct the eikonal terms $\bar{f}_{En}$ in a consistent way beyond the leading correction, of order k^{-1}. However, in view of the difficulties involved in generalising the Wallace approach to the multichannel situation, we do not consider these additional phase corrections. Instead, we are only interested in the leading correction to $\bar{f}_{En}$ (of order k^{-1}) arising from $\chi_1(\boldsymbol{b})$. We note that this leading correction may equally be obtained from the modified Wallace amplitude

$$\tilde{f}_W=\frac{k}{2\pi i}\int d^2\boldsymbol{b}\exp(i\boldsymbol{\Delta}\cdot\boldsymbol{b})[\exp(ik^{-1}\chi_0(\boldsymbol{b}))(1+ik^{-3}\chi_1(\boldsymbol{b}))-1]. \tag{2.4}$$

Indeed, by expanding $\tilde{f}_W$ in powers of the interaction potential, we generate a series whose general term is identical to $\bar{f}_{Wn}$, apart from corrections of relative order k^{-2} (such as $\chi_0^{n-4}\chi_1^2$) beginning at $n=4$. Since, as pointed out in I, these correction terms lead to divergent integrals when the term $\bar{f}_{Wn}$ is generalised to the many-body case (such as $e^{\pm}$-H collisions), it is reasonable to consider the modified Wallace amplitude $\tilde{f}_W$ given by equation (2.4)—which does not contain these correction terms—as a good alternative starting point for the UEBS method. We also remark that the potential scattering amplitude $\tilde{f}_W$ is unitary through first order in χ_1 and through order k^{-3}.

Before generalising the modified Wallace amplitude $\tilde{f}_W$ of equation (2.4) to the multichannel case, we have made an extensive comparison of this approximation with that based on the Wallace amplitude f_W of equation (2.1), as well as with other related approximations (first Born amplitude $\bar{f}_{B1}$, second Born amplitude $f_{B2}=\bar{f}_{B1}+\bar{f}_{B2}$, eikonal amplitude f_E, eikonal-Born series amplitudes $f_{EBS}=\bar{f}_{B1}+\bar{f}_{B2}+\bar{f}_{E3}$ and $f_{EBS'}=f_E-\bar{f}_{E2}+\bar{f}_{B2}$) and with the exact results (obtained by using the partial-wave method) for a variety of 'Yukawa-type' interactions (see equation (2.14) of I). As an example, we show in table 1 the differential cross section for scattering of electrons and positrons by the static potential of the ground-state hydrogen atom, at an incident projectile energy of 100 eV ($k=2.71$). As seen from this table, both amplitudes f_W and $\tilde{f}_W$ give differential cross sections in close agreement with each other and with the exact values, for electrons as well as positrons, and for the entire angular range. We also note from table 1 that the values obtained by using the modified Wallace amplitude $\tilde{f}_W$ are still more accurate than those corresponding to the amplitude f_W; this result is typical of what we found in studying a variety of other cases. It is also interesting to remark from table 1 that the EBS method gives very good results for the case of incident electrons. In fact, at large scattering angles, where terms of higher order (in k^{-1}) than Re $\bar{f}_{B3}$—which are not included in the EBS amplitude—have significant magnitudes, the accuracy of the EBS method depends delicately on cancellations between these higher-order terms (Byron and Joachain 1973). Although present in the case studied in table 1 for incident electrons, these cancellations cannot be expected to occur in

Table 1. Differential cross sections (in au) for scattering of electrons (charge $Q=-1$) and positrons ($Q=1$) by the static potential of the ground-state hydrogen atom $V(r)=Q(1+1/r)\exp(-2r)$, at an incident electron energy of 100 eV (three significant figures are given. Powers of ten are denoted by a superscript). B1, first Born approximation; B2, second Born approximation; E, eikonal approximation; EBS and EBS′, eikonal-Born series approximations (see text); W and $\tilde{\text{W}}$, Wallace approximations (see text) compared with the exact results.

θ (deg)	B1	B2	E	EBS	EBS′	W	$\tilde{\text{W}}$	Exact
Electrons								
0	1.00	1.15	9.23^{-1}	1.01	1.02	1.01	1.01	1.02
30	3.13^{-1}	3.95^{-1}	2.81^{-1}	3.22^{-1}	3.23^{-1}	3.19^{-1}	3.20^{-1}	3.28^{-1}
60	5.68^{-2}	8.89^{-2}	5.03^{-2}	6.20^{-2}	6.02^{-2}	6.03^{-2}	6.07^{-2}	6.39^{-2}
90	1.69^{-2}	3.23^{-2}	1.52^{-2}	2.01^{-2}	1.81^{-2}	1.88^{-2}	1.89^{-2}	2.05^{-2}
120	7.84^{-3}	1.72^{-2}	7.21^{-3}	1.02^{-2}	8.47^{-3}	9.04^{-3}	9.13^{-3}	1.01^{-2}
150	5.14^{-3}	1.22^{-2}	4.78^{-3}	7.09^{-3}	5.54^{-3}	6.03^{-3}	6.10^{-3}	6.80^{-3}
180	4.50^{-3}	1.09^{-2}	4.19^{-3}	6.33^{-3}	4.84^{-3}	5.30^{-3}	5.36^{-3}	6.00^{-3}
Positrons								
0	1.00	9.38^{-1}	9.23^{-1}	8.16^{-1}	8.21^{-1}	8.39^{-1}	8.41^{-1}	8.56^{-1}
30	3.13^{-1}	2.99^{-1}	2.81^{-1}	2.37^{-1}	2.37^{-1}	2.45^{-1}	2.46^{-1}	2.52^{-1}
60	5.68^{-2}	6.31^{-2}	5.02^{-2}	4.24^{-2}	3.98^{-2}	4.07^{-2}	4.11^{-2}	4.26^{-2}
90	1.69^{-2}	2.33^{-2}	1.52^{-2}	1.46^{-2}	1.22^{-2}	1.18^{-2}	1.20^{-2}	1.26^{-2}
120	7.84^{-3}	1.28^{-2}	7.21^{-3}	8.02^{-3}	5.97^{-3}	5.51^{-3}	5.60^{-3}	5.91^{-3}
150	5.14^{-3}	9.26^{-3}	4.78^{-3}	5.87^{-3}	4.05^{-3}	3.63^{-3}	3.69^{-3}	3.90^{-3}
180	4.50^{-3}	8.34^{-3}	4.19^{-3}	5.32^{-3}	3.58^{-3}	3.18^{-3}	3.23^{-3}	3.42^{-3}

general; indeed, it is seen from table 1 that at the same energy they are not present for the case of incident positrons.

2.2. *The unitarised eikonal-Born series amplitude for direct electron-atom and positron-atom collisions*

2.2.1. Basic equations. Let us now consider the scattering of an electron or positron by a neutral target atom containing Z electrons. In our previous work (Byron *et al* 1981, 1982) we reported results for the 1s-1s and 1s-2s transitions in $e^{\pm}$-H collisions using the direct UEBS amplitude

$$f_{\text{UEBS}}=f_{\text{W}}-\bar{f}_{\text{W2}}+\bar{f}_{\text{B2}} \tag{2.5}$$

where f_{W} denotes the many-body Wallace amplitude (see equation (3) of Byron *et al* 1981), $\bar{f}_{\text{W2}}$ is the second term of the corresponding Wallace series (obtained by expanding f_{W} in powers of the direct projectile-target interaction V_{d}) and $\bar{f}_{\text{B2}}$ is the second term of the Born series. In the present work we have also calculated the amplitude (2.5) for the 1s-2p transition. However, because of the difficulties arising in the many-body Wallace term $\bar{f}_{\text{W}n}$ (with $n\geqslant 4$) due to corrections of relative order k_i^{-2} involving powers of χ_1 higher than the first, and in view of the results reported in § 2.1 for potential scattering, we have been led to analyse the new UEBS amplitude

$$\tilde{f}_{\text{UEBS}}=\tilde{f}_{\text{W}}-\bar{f}_{\text{W2}}+\bar{f}_{\text{B2}} \tag{2.6}$$

where $\tilde{f}_{\text{W}}$ is the many-body generalisation of equation (2.4). For a transition $|\boldsymbol{k}_i, 0\rangle\rightarrow$

$|\boldsymbol{k}_f, m\rangle$ (where $|0\rangle$ and $|m\rangle$ are the initial and final target states, respectively) this quantity reads

$$\tilde{f}_{\mathrm{W}}=\frac{k_i}{2\pi\mathrm{i}}\int \mathrm{d}^2 b \exp(\mathrm{i}\boldsymbol{\Delta}\cdot\boldsymbol{b})\langle\psi_m(X)|[\exp(\mathrm{i}k_i^{-1}\chi_0(\boldsymbol{b}, X))(1+\mathrm{i}k_i^{-3}\chi_1(\boldsymbol{b}, X))-1]|\psi_0(X)\rangle \tag{2.7}$$

where the symbol X denotes all the target coordinates, $\psi_n(X)$ is the wavefunction corresponding to the target state $|n\rangle$ in the coordinate representation, χ_0 is the Glauber phase (see equation (3.8) of I) and χ_1 the leading Wallace correction to it, which is of second order in the direct projectile-target interaction potential (see equation (3.9) of I). The incident particle coordinate $\boldsymbol{r}_0$ has been written $\boldsymbol{r}_0=\boldsymbol{b}+z\hat{\boldsymbol{n}}$, where $\hat{\boldsymbol{n}}$ is perpendicular to the momentum transfer $\boldsymbol{\Delta}$. It is important to note that, as in the case of potential scattering considered above, the terms of the Wallace series, obtained by expanding the amplitudes f_{W} and $\tilde{f}_{\mathrm{W}}$ in powers of the interaction potential V_{d}, are identical up to and including the third-order term $\bar{f}_{\mathrm{W}3}$.

For the case of an atomic hydrogen target one has

$$\chi_0=-Q\ln(\beta^2/b^2) \tag{2.8}$$

where $Q=+1$ for positrons and -1 for electrons; the coordinate $\boldsymbol{r}_1$ of the target electron has been written $\boldsymbol{r}_1=\boldsymbol{b}_1+z_1\hat{\boldsymbol{n}}$, and $\boldsymbol{\beta}=\boldsymbol{b}-\boldsymbol{b}_1$. In this case the Wallace phase correction χ_1 can also be obtained in closed form (Byron *et al* 1981, 1982) and is given by

$$\chi_1=\frac{Q^2\pi}{(b\beta)^{1/2}}\left[P_{-1/2}\left(\frac{b^2+\beta^2+z_1^2}{2b\beta}\right)-\hat{\boldsymbol{b}}\cdot\hat{\boldsymbol{\beta}}P_{1/2}\left(\frac{b^2+\beta^2+z_1^2}{2b\beta}\right)\right] \tag{2.9}$$

where $P_{1/2}$ and $P_{-1/2}$ are Legendre functions. In the present paper we shall report results obtained for the 1s–1s, 1s–2s and 1s–2p transitions in atomic hydrogen using the 'new' UEBS direct amplitude (2.6). For the purpose of comparison we shall also give results obtained from the 'old' UEBS direct amplitude (2.5) as well as from the Glauber amplitude f_{G} (see equation (3.12) of I), the Wallace amplitude f_{W} and the modified Wallace amplitude $\tilde{f}_{\mathrm{W}}$.

2.2.2. The large momentum transfer limit. In order to analyse the behaviour of the UEBS amplitude (2.6) in the limit of large momentum transfers, one must study the second Born term $\bar{f}_{\mathrm{B}2}$ as well as the quantities $\tilde{f}_{\mathrm{W}}$ and $\bar{f}_{\mathrm{W}2}$ in this limit. The large momentum transfer behaviour of $\bar{f}_{\mathrm{B}2}$ has been analysed for the 1s–1s transition by Byron and Joachain (1973) and for the 1s–2s and 1s–2p transitions by Byron and Latour (1976). A general discussion of the k and Δ dependence of the terms $\bar{f}_{\mathrm{B}n}$ of the Born series for elastic and inelastic s–s transitions has been given by Byron and Joachain (1977). We therefore concentrate here on the large momentum transfer behaviour of the Wallace-type quantities $\tilde{f}_{\mathrm{W}}$ and $\bar{f}_{\mathrm{W}2}$. In fact, using a generalisation of the method used in I for the elastic scattering case, we shall study the large-Δ limit of the amplitude $\tilde{f}_{\mathrm{W}}$ through *third order* in perturbation theory. Since the two amplitudes f_{W} and $\tilde{f}_{\mathrm{W}}$ agree exactly through that order, it is immaterial whether one starts from the expression of $\tilde{f}_{\mathrm{W}}$ or from that of f_{W} if one is interested only in the terms $\bar{f}_{\mathrm{W}n}$ with $n=1, 2, 3$. In order to make contact most easily with the method developed in I, we shall use here the many-body Wallace amplitude f_{W}.

As stated in I, the large-Δ behaviour of f_{W} is controlled by the small-b behaviour of the phases χ_0 and χ_1. For $e^{\pm}$-H collisions, we have from equation (2.8), for small values of b

$$\chi_0 \simeq Q \ln b^2 - Q \ln b_1^2 + \mathrm{O}(b) \tag{2.10}$$

and from equation (2.9) we find that

$$\chi_1 \simeq Q^2\bigg(\frac{2r_1\cos(\phi_1-\phi)}{b_1}\frac{1}{b}-\frac{1}{r_1}\ln b^2+\frac{2}{r_1}\ln\frac{4r_1^2}{b_1}$$
$$-\frac{2}{r_1}\sin^2(\phi_1-\phi)+\frac{2z_1^2}{b_1^2 r_1}\cos 2(\phi_1-\phi)\bigg)+\mathrm{O}(b). \tag{2.11}$$

This last equation supersedes equation (4.12) of I, in which terms involving the azimuthal angle ϕ_1, unimportant for the 1s–1s transition studied in I, were omitted.

Upon substitution of equations (2.10) and (2.11) in the many-body Wallace amplitude f_W, we have for large Δ

$$f_\mathrm{W} \simeq \frac{k_i}{2\pi \mathrm{i}}\int \mathrm{d}^2\boldsymbol{b}\exp(\mathrm{i}\boldsymbol{\Delta}\cdot\boldsymbol{b})\bigg\langle\psi_m(\boldsymbol{r}_1)\bigg|\bigg\{\exp\bigg[\mathrm{i}\bigg(\frac{Q}{k_i}\ln b^2-\frac{Q}{k_i}\ln b_1^2$$
$$-\frac{Q^2}{k_i^3 r_1}\ln b^2+\frac{2Q^2}{k_i^3 r_1}\ln\frac{4r_1^2}{b_1}-\frac{2Q^2}{k_i^3 r_1}\sin^2(\phi_1-\phi)$$
$$+\frac{2Q^2 z_1^2}{k_i^3 b_1^2 r_1}\cos 2(\phi_1-\phi)+\frac{2Q^2 r_1}{k_i^3 b b_1}\cos(\phi_1-\phi)\bigg)\bigg]-1\bigg\}\bigg|\psi_0(\boldsymbol{r}_1)\bigg\rangle. \tag{2.12}$$

Let us begin by considering s–s transitions. If we expand the exponential in equation (2.12) and keep terms only through order Q^3, then the integral on ϕ_1 will eliminate the last two terms in the exponential and replace $\sin^2(\phi_1-\phi)$ by $\frac{1}{2}$. The integration on $\mathrm{d}^2\boldsymbol{b}$ is then readily done to yield the following large-Δ behaviour:

$$\bar{f}_\mathrm{W1} \simeq -(2Q/\Delta^2)\langle\psi_m|\psi_0\rangle \tag{2.13a}$$
$$\mathrm{Re}\,\bar{f}_\mathrm{W2} \simeq (2Q^2/k_i^2\Delta^2)\langle\psi_m|r_1^{-1}|\psi_0\rangle \tag{2.13b}$$
$$\mathrm{Im}\,\bar{f}_\mathrm{W2} \simeq (4Q^2/k_i\Delta^2)\langle\psi_m|\ln b_1+\ln\tfrac{1}{2}\Delta+\gamma|\psi_0\rangle \tag{2.13c}$$
$$\mathrm{Re}\,\bar{f}_\mathrm{W3} \simeq (4Q^3/k_i^2\Delta^2)\langle\psi_m|(\ln b_1+\ln\tfrac{1}{2}\Delta+\gamma)^2|\psi_0\rangle \tag{2.13d}$$
$$\mathrm{Im}\,\bar{f}_\mathrm{W3} \simeq -(8Q^3/k_i^3\Delta^2)\langle\psi_m|(\ln r_1+\ln\Delta+\gamma-\tfrac{1}{4})r_1^{-1}|\psi_0\rangle \tag{2.13e}$$

where $\gamma = 0.577\,215\,66\ldots$ is Euler's constant.

For elastic scattering from the ground state, the above expressions yield

$$\bar{f}_\mathrm{W1} \simeq -2Q/\Delta^2 \tag{2.14a}$$
$$\mathrm{Re}\,\bar{f}_\mathrm{W2} \simeq 2Q^2/k_i^2\Delta^2 \tag{2.14b}$$
$$\mathrm{Im}\,\bar{f}_\mathrm{W2} \simeq (4Q^2/k_i\Delta^2)(\ln\tfrac{1}{2}\Delta+\tfrac{1}{2}) \tag{2.14c}$$
$$\mathrm{Re}\,\bar{f}_\mathrm{W3} \simeq (4Q^3/k_i^2\Delta^2)(\ln^2\tfrac{1}{2}\Delta+\ln\tfrac{1}{2}\Delta+\tfrac{1}{12}\pi^2) \tag{2.14d}$$
$$\mathrm{Im}\,\bar{f}_\mathrm{W3} \simeq -(8Q^3/k_i^3\Delta^2)(\ln\tfrac{1}{2}\Delta+\tfrac{3}{4}) \tag{2.14e}$$

which are the results found in I, except that the expression (2.14e) for $\mathrm{Im}\,\bar{f}_\mathrm{W3}$ supersedes equation (4.17e) of I, where a detailed discussion of the above results is given. We recall that equations (2.14b) and (2.14c) for $\bar{f}_\mathrm{W2}$ agree exactly with the large-Δ behaviour of $\bar{f}_\mathrm{B2}$, so the large momentum transfer dependence of $\tilde{f}_\mathrm{UEBS}$ is identical to that of $\bar{f}_{\mathrm{W}}$. Moreover, as will be shown below, the part of $\mathrm{Im}\,\bar{f}_{\mathrm{W}3}$ in equation (2.14e) proportional to $\ln\Delta$ is exactly the leading term of $\mathrm{Im}\,\bar{f}_{\mathrm{B}3}$.

For 1s–2s transitions, we find from equations (2.13) that for large Δ

$$\bar{f}_{\mathrm{W}1}\simeq 0 \tag{2.15a}$$

$$\mathrm{Re}\,\bar{f}_{\mathrm{W}2}\simeq 8\sqrt{2}\,Q^2/27k_i^2\Delta^2 \tag{2.15b}$$

$$\mathrm{Im}\,\bar{f}_{\mathrm{W}2}\simeq -64\sqrt{2}\,Q^2/81k_i\Delta^2 \tag{2.15c}$$

$$\mathrm{Re}\,\bar{f}_{\mathrm{W}3}\simeq -(128\sqrt{2}\,Q^3/81k_i^2\Delta^2)(\ln\tfrac{2}{3}\Delta+\tfrac{1}{2}) \tag{2.15d}$$

$$\mathrm{Im}\,\bar{f}_{\mathrm{W}3}\simeq -(32\sqrt{2}\,Q^3/27k_i^3\Delta^2)(\ln\tfrac{2}{3}\Delta-\tfrac{1}{4}). \tag{2.15e}$$

The difference between equations (2.14a) and (2.15a) is striking, and results from the fact that the asymptotic method we have used does not yield terms which fall off faster than Δ^{-2}. Since the term $\bar{f}_{\mathrm{W}1}$ (which is equal to the first Born term $\bar{f}_{\mathrm{B}1}$) falls off like Δ^{-6} for all 1s–ns inelastic transitions, we find here that $\bar{f}_{\mathrm{W}1}\simeq 0$. The terms $\mathrm{Im}\,\bar{f}_{\mathrm{W}2}$ and $\mathrm{Re}\,\bar{f}_{\mathrm{W}3}$, given respectively by equations (2.15c) and (2.15d), duplicate the large-Δ behaviour of the corresponding terms of the Glauber series, as in the elastic scattering case. The term $\mathrm{Re}\,\bar{f}_{\mathrm{W}2}$ (which is missing from the Glauber series), as given by equation (2.15b), agrees exactly with the large-Δ expression of $\mathrm{Re}\,\bar{f}_{\mathrm{B}2}$ found by Byron and Latour (1976), so that again the large-Δ behaviour of $\bar{f}_{\mathrm{UEBS}}$ is the same as that of $\bar{f}_{\mathrm{W}}$. Finally, we note that the term $\mathrm{Im}\,\bar{f}_{\mathrm{W}3}$ (see equation (2.15e)) is also missing from the Glauber series. As in the elastic scattering case, the part of $\mathrm{Im}\,\bar{f}_{\mathrm{W}3}$ which is proportional to $\ln\Delta$ agrees exactly with the large-Δ expression of the term $\mathrm{Im}\,\bar{f}_{\mathrm{B}3}$ obtained below from the unitarity relations.

Let us now consider s–p transitions. Returning to our large-Δ equation (2.12) for f_{W}, we see that if ψ_m is a p state then upon expanding the exponential in powers of Q we have

$$\bar{f}_{\mathrm{W}1}\simeq 0 \tag{2.16a}$$

$$\bar{f}_{\mathrm{W}2}\simeq\frac{Q^2}{\pi k_i^2}\int \mathrm{d}^2\boldsymbol{b}\,\exp(\mathrm{i}\boldsymbol{\Delta}\cdot\boldsymbol{b})\left\langle\psi_m(\boldsymbol{r}_1)\left|\frac{r_1}{bb_1}\cos(\phi_1-\phi)\right|\psi_0(\boldsymbol{r}_1)\right\rangle \tag{2.16b}$$

$$\bar{f}_{\mathrm{W}3}\simeq\mathrm{i}\frac{2Q^3}{\pi k_i^3}\int \mathrm{d}^2\boldsymbol{b}\,\exp(\mathrm{i}\boldsymbol{\Delta}\cdot\boldsymbol{b})$$
$$\times\left\langle\psi_m(\boldsymbol{r}_1)\left|(\ln b-\ln b_1)\frac{r_1}{bb_1}\cos(\phi_1-\phi)\right|\psi_0(\boldsymbol{r}_1)\right\rangle. \tag{2.16c}$$

As in the case of inelastic s–s transitions, our asymptotic method, which does not give terms falling off faster than Δ^{-2}, yields the result $\bar{f}_{\mathrm{W}1}\simeq 0$. In fact, for 1s–$n$p transitions, the term $\bar{f}_{\mathrm{W}1}$ $(=\bar{f}_{\mathrm{B}1})$ falls off like Δ^{-7}. Furthermore, for 1s–2pm transitions we find from equation (2.16b) that the second term of the Wallace series is given by

$$\begin{aligned}\bar{f}_{\mathrm{W}2}&\simeq\mp\mathrm{i}\frac{16Q^2}{27k_i^2\Delta}\exp(\mp\mathrm{i}\phi_\Delta) && m=\pm1\\ &=0 && m=0\end{aligned} \tag{2.17}$$

where ϕ_Δ denotes the azimuthal angle of the momentum transfer $\boldsymbol{\Delta}$. We recall that in evaluating eikonal expressions the Z axis is taken to be perpendicular to $\boldsymbol{\Delta}$ $(\theta_\Delta=\pi/2)$.

If we write the Cartesian components of the unit vector $\hat{\boldsymbol{\Delta}}$ along the momentum transfer as

$$\hat{\Delta}_x = (4\pi/3)^{1/2} 2^{-1/2} (Y^*_{1,-1}(\pi/2, \phi_\Delta) - Y^*_{1,1}(\pi/2, \phi_\Delta)) \tag{2.18a}$$

$$\hat{\Delta}_y = (4\pi/3)^{1/2} (-\mathrm{i}) 2^{-1/2} (Y^*_{1,-1}(\pi/2, \phi_\Delta) + Y^*_{1,1}(\pi/2, \phi_\Delta)) \tag{2.18b}$$

$$\hat{\Delta}_z = (4\pi/3)^{1/2} Y^*_{1,0}(\pi/2, \phi_\Delta) = 0 \tag{2.18c}$$

we can recast equation (2.17) into the form

$$\bar{f}_{W2} \simeq \mathrm{i}\frac{16\sqrt{2}\,Q^2}{27 k_i^2 \Delta}\hat{\boldsymbol{\Delta}}. \tag{2.19}$$

Now, since (2.19) is a vector equation, it holds in any coordinate system, provided $\hat{\boldsymbol{\Delta}}$ is interpreted as the unit vector along the momentum transfer in that frame. In particular, equation (2.19) is valid in the coordinate system in which the Z axis lies along the incident momentum $\boldsymbol{k}_i$; this is the frame in which our theoretical results will be compared with experimental data in § 3. We note from equation (2.19) that $\bar{f}_{W2}$ does not contain any real part, since our asymptotic method does not give terms which fall off faster than Δ^{-2}. In fact, the real part of $\bar{f}_{W2}$ is just the Glauber part, which can be readily evaluated in closed form to give

$$\mathrm{Re}\,\bar{f}_{W2} \simeq \frac{32\sqrt{2}}{27 k_i \Delta^3}\hat{\boldsymbol{\Delta}}. \tag{2.20}$$

The result (2.19) agrees exactly with the large-Δ behaviour of the imaginary part of the second Born term for that process, $\bar{f}_{B2}$, obtained by Byron and Latour (1976). This is the leading contribution in second order. However, the expression (2.20) for $\mathrm{Re}\,\bar{f}_{W2}$ does not agree with the corresponding expression for $\mathrm{Re}\,\bar{f}_{B2}$ (see equation (4.10) of Byron and Latour (1976)). Thus in the case of s–p transitions it is even more important to replace the term $\bar{f}_{W2}$ by $\bar{f}_{B2}$, as is done in constructing the UEBS amplitude.

The third-order Wallace term (2.16c) can be evaluated in a similar way for 1s–2pm transitions. The result is

$$\bar{f}_{W3} \simeq \frac{32\sqrt{2}\,Q^3}{27 k_i^3 \Delta}(\ln \tfrac{2}{3}\Delta + \tfrac{5}{6})\hat{\boldsymbol{\Delta}}. \tag{2.21}$$

This expression is purely real for the reason mentioned above; the imaginary part of $\bar{f}_{W3}$ (the Glauber part) can be shown to behave like Δ^{-3} for large Δ, as was the case for the Glauber part of $\bar{f}_{W2}$.

2.2.3. Unitarity relations and the structure of the third Born term. Let us start from the general unitarity relations for the T matrix (Joachain 1983)

$$\mathrm{i}[T_{ba} - T^*_{ab}] = 2\pi \sum_n \delta(E - E_n)\delta(\boldsymbol{P} - \boldsymbol{P}_n) T_{bn} T^*_{an}. \tag{2.22}$$

In terms of the scattering amplitude for the transition from $a = (\boldsymbol{k}_i, n_i)$ to $b = (\boldsymbol{k}_f, n_f)$, which we write explicitly as $f(\boldsymbol{k}_f, n_f; \boldsymbol{k}_i, n_i)$, we have

$$f(\boldsymbol{k}_f, n_f; \boldsymbol{k}_i, n_i) - f^*(\boldsymbol{k}_i, n_i; \boldsymbol{k}_f, n_f) = 2\mathrm{i}\sum_n \frac{k_n}{4\pi}\int \mathrm{d}\hat{\boldsymbol{q}}\, f(\boldsymbol{k}_f, n_f; \boldsymbol{k}_n, n) f^*(\boldsymbol{k}_i, n_i; \boldsymbol{k}_n, n) \tag{2.23}$$

where $k_n^2 = k_i^2 + 2(w_i - w_n)$ and $\boldsymbol{k}_n = k_n \hat{\boldsymbol{q}}$.

Expanding in powers of the interaction potential, we obtain in third order

$$\bar{f}_{B3}(\boldsymbol{k}_f, n_f; \boldsymbol{k}_i, n_i) - \bar{f}^*_{B3}(\boldsymbol{k}_i, n_i; \boldsymbol{k}_f, n_f)$$
$$= 2\mathrm{i} \sum_n \frac{k_n}{4\pi} \int \mathrm{d}\hat{\boldsymbol{q}}[\bar{f}_{B2}(\boldsymbol{k}_f, n_f; \boldsymbol{k}_n, n)\bar{f}^*_{B1}(\boldsymbol{k}_i, n_i; \boldsymbol{k}_n, n)$$
$$+ \bar{f}_{B1}(\boldsymbol{k}_f, n_f; \boldsymbol{k}_n, n)\bar{f}^*_{B2}(\boldsymbol{k}_i, n_i; \boldsymbol{k}_n, n)]. \tag{2.24}$$

Let us first consider the case in which n_i and n_f are both s states of the target. We may then use the microreversibility theorem (along with the fact that the amplitude for s–s transitions can depend only on k_i and Δ) to rewrite equation (2.24) as

$$\mathrm{Im}\, \bar{f}_{B3}(\boldsymbol{k}_f, n_f; \boldsymbol{k}_i, n_i)$$
$$= \sum_n \frac{k_n}{4\pi} \int \mathrm{d}\hat{\boldsymbol{q}}[\bar{f}_{B2}(\boldsymbol{k}_f, n_f; \boldsymbol{k}_n, n)\bar{f}^*_{B1}(\boldsymbol{k}_i, n_i; \boldsymbol{k}_n, n)$$
$$+ \bar{f}_{B1}(\boldsymbol{k}_f, n_f; \boldsymbol{k}_n, n)\bar{f}^*_{B2}(\boldsymbol{k}_i, n_i; \boldsymbol{k}_n, n)]. \tag{2.25}$$

If we restrict our attention to the region of large momentum transfers, the dominant term is obtained when the amplitudes in the summation fall off as slowly as possible with increasing intermediate momentum transfers $\boldsymbol{\Delta}_i = \boldsymbol{k}_i - \boldsymbol{k}_n$ and $\boldsymbol{\Delta}_f = \boldsymbol{k}_f - \boldsymbol{k}_n$. This happens for the first term in square brackets when $n = n_i$ and for the second term when $n = n_f$, since then both $\bar{f}_{B1}$ and $\bar{f}_{B2}$ fall off like the inverse square of the intermediate momentum transfer. For all other intermediate states, the first Born term falls off at least as rapidly as the inverse sixth power of the intermediate momentum transfer. Thus, we may write in the limit of large momentum transfers

$$\mathrm{Im}\, \bar{f}_{B3}(\boldsymbol{k}_f, n_f; \boldsymbol{k}_i, n_i)$$
$$\simeq \frac{k_i}{4\pi} \int \mathrm{d}\hat{\boldsymbol{q}}[\bar{f}_{B2}(\boldsymbol{k}_f, n_f; \boldsymbol{q}, n_i)\bar{f}^*_{B1}(\boldsymbol{k}_i, n_i; \boldsymbol{q}, n_i)]_{q=k_i}$$
$$+ \frac{k_f}{4\pi} \int \mathrm{d}\hat{\boldsymbol{q}}[\bar{f}_{B1}(\boldsymbol{k}_f, n_f; \boldsymbol{q}, n_f)\bar{f}^*_{B2}(\boldsymbol{k}_i, n_i; \boldsymbol{q}, n_f)]_{q=k_f}. \tag{2.26}$$

Since for elastic scattering $\bar{f}_{B1}$ is purely real, the contribution to the right-hand side of equation (2.26) coming from the imaginary part of $\bar{f}_{B2}$ must vanish identically, and it is straightforward to show that this is indeed the case. Thus, equation (2.26) may be rewritten as

$$\mathrm{Im}\, \bar{f}_{B3}(\boldsymbol{k}_f, n_f; \boldsymbol{k}_i, n_i)$$
$$\simeq \frac{k_i}{4\pi} \int \mathrm{d}\hat{\boldsymbol{q}}[\mathrm{Re}\, \bar{f}_{B2}(\boldsymbol{k}_f, n_f; \boldsymbol{q}, n_i)\bar{f}_{B1}(\boldsymbol{k}_i, n_i; \boldsymbol{q}, n_i)]_{q=k_i}$$
$$+ \frac{k_f}{4\pi} \int \mathrm{d}\hat{\boldsymbol{q}}[\bar{f}_{B1}(\boldsymbol{k}_f, n_f; \boldsymbol{q}, n_f)\, \mathrm{Re}\, \bar{f}_{B2}(\boldsymbol{k}_i, n_i; \boldsymbol{q}, n_f)]_{q=k_f} \tag{2.27}$$

which we shall refer to as the 'generalised elastic unitarity' relation for s–s transitions.

For the case of s–s transitions and for large $k_i(\simeq k_f)$ and large Δ, the integrand in each term on the right-hand side of equation (2.27) is of the form $[k_i^2(\Delta_f^2 + \beta^2)(\Delta_i^2 + \alpha^2)]^{-1}$ where now $\boldsymbol{\Delta}_i = \boldsymbol{k}_i - \boldsymbol{q}$ and $\boldsymbol{\Delta}_f = \boldsymbol{k}_f - \boldsymbol{q}$. The relevant integrals can then be performed by using the results given in Appendix A of Byron and Joachain (1977). One obtains for the 1s–1s transition

$$\mathrm{Im}\,\bar{f}_{\mathrm{B3}}(1\mathrm{s}, 1\mathrm{s}) \simeq -(8Q^3/k_i^3\Delta^2)\ln\Delta \tag{2.28}$$

and for the 1s–2s transition

$$\mathrm{Im}\,\bar{f}_{\mathrm{B3}}(2\mathrm{s}, 1\mathrm{s}) \simeq -(32\sqrt{2}\,Q^3/27k_i^3\Delta^2)\ln\Delta. \tag{2.29}$$

It is gratifying to note that the leading terms of $\mathrm{Im}\,\bar{f}_{\mathrm{W3}}$, proportional to $\Delta^{-2}\ln\Delta$ in equations (2.14*e*) and (2.15*e*), agree exactly with the results (2.28) and (2.29), respectively. We remark that the part of $\mathrm{Im}\,\bar{f}_{\mathrm{B3}}$ proportional simply to Δ^{-2} is not given correctly by the generalised elastic unitarity relation (2.27). In order to obtain that part, an infinite number of intermediate states must be retained in equation (2.25).

Turning now to the case of s–p transitions, it is straightforward to show, using a method similar to the one employed above for s–s transitions, that in the large momentum transfer region we have

$$\begin{aligned}\mathrm{Re}\,\bar{f}_{\mathrm{B3}}(\boldsymbol{k}_f, n_f; \boldsymbol{k}_i, n_i)&\\ \simeq -\frac{k_i}{4\pi}&\int \mathrm{d}\hat{\boldsymbol{q}}[\mathrm{Im}\,\bar{f}_{\mathrm{B2}}(\boldsymbol{k}_f, n_f; \boldsymbol{q}, n_i)\bar{f}_{\mathrm{B1}}(\boldsymbol{k}_i, n_i; \boldsymbol{q}, n_i)]_{q=k_i}\\ -\frac{k_f}{4\pi}&\int \mathrm{d}\hat{\boldsymbol{q}}[\bar{f}_{\mathrm{B1}}(\boldsymbol{k}_f, n_f; \boldsymbol{q}, n_f)\,\mathrm{Im}\,\bar{f}_{\mathrm{B2}}(\boldsymbol{k}_i, n_i; \boldsymbol{q}, n_f)]_{q=k_f}.\end{aligned} \tag{2.30}$$

Making use of the large momentum transfer behaviour of $\mathrm{Im}\,\bar{f}_{\mathrm{B2}}$ and $\bar{f}_{\mathrm{B1}}$ one finds for the 1s–2p transition

$$\mathrm{Re}\,\bar{f}_{\mathrm{B3}}(2\mathrm{p}, 1\mathrm{s}) \simeq (32\sqrt{2}\,Q^3/27k_i^3\Delta)(\ln\Delta)\hat{\boldsymbol{\Delta}}. \tag{2.31}$$

This agrees exactly with the term in $\ln\Delta$ found in equation (2.21) for $\bar{f}_{\mathrm{W3}}(2\mathrm{p}, 1\mathrm{s})$. As in the case of s–s transitions, it would be necessary to retain an infinite number of terms in equation (2.24) in order to obtain the term proportional to $k_i^{-3}\Delta^{-1}$.

2.3. *The exchange amplitude*

In I, exact relationships (equations (3.29) and (3.36)) were derived for obtaining exchange amplitudes. For a transition $(\boldsymbol{k}_i, n_i) \to (\boldsymbol{k}_f, n_f)$ these relationships read

$$\begin{aligned}g(\boldsymbol{k}_f, n_f; \boldsymbol{k}_i, n_i) &= g_{\mathrm{B1}}(\boldsymbol{k}_f, n_f; \boldsymbol{k}_i, n_i)\\ &+ (2\pi^2)^{-1}\sum_n \int \mathrm{d}\boldsymbol{q}\frac{1}{q^2 - k_n^2 - \mathrm{i}\varepsilon}\, g_{\mathrm{B1}}(\boldsymbol{k}_f, n_f; \boldsymbol{q}, n) f(\boldsymbol{q}, n; \boldsymbol{k}_i, n_i)\end{aligned} \tag{2.32a}$$

and

$$\begin{aligned}g(\boldsymbol{k}_f, n_f; \boldsymbol{k}_i, n_i) &= g_{\mathrm{B1}}(\boldsymbol{k}_f, n_f; \boldsymbol{k}_i, n_i)\\ &+ (2\pi^2)^{-1}\sum_n \int \mathrm{d}\boldsymbol{q}\frac{1}{q^2 - k_n^2 - \mathrm{i}\varepsilon} f(\boldsymbol{k}_f, n_f; \boldsymbol{q}, n) g_{\mathrm{B1}}(\boldsymbol{q}, n; \boldsymbol{k}_i, n_i)\end{aligned} \tag{2.32b}$$

where f is the direct amplitude and g_{B1} is the first Born exchange amplitude. In I an 'elastic', non-perturbative approximation to (2.32) was given, and applied to the 1s–1s transition in atomic hydrogen. For the case of the 1s–2s transition, the corresponding equation is

$$g_{\mathrm{UEBS}}(\boldsymbol{k}_f, 2\mathrm{s}; \boldsymbol{k}_i, 1\mathrm{s})$$
$$= g_{\mathrm{B1}}^{(01)}(\boldsymbol{k}_f, 2\mathrm{s}, \boldsymbol{k}_i, 1\mathrm{s})$$
$$+(2\pi^2)^{-1} \int \mathrm{d}\boldsymbol{q} \frac{1}{q^2 - k_i^2 - \mathrm{i}\varepsilon} g_{\mathrm{B1}}^{(01)}(\boldsymbol{k}_f, 2\mathrm{s}, \boldsymbol{q}, 1\mathrm{s}) f_{\mathrm{UEBS}}(\boldsymbol{q}, 1\mathrm{s}; \boldsymbol{k}_i, 1\mathrm{s})$$
$$+(2\pi^2)^{-1} \int \mathrm{d}\boldsymbol{q} \frac{1}{q^2 - k_f^2 - \mathrm{i}\varepsilon} g_{\mathrm{B1}}^{(01)}(\boldsymbol{k}_f, 2\mathrm{s}, \boldsymbol{q}, 2\mathrm{s}) f_{\mathrm{UEBS}}(\boldsymbol{q}, 2\mathrm{s}, \boldsymbol{k}_i, 1\mathrm{s})$$
$$+(2\pi^2)^{-1} \int \mathrm{d}\boldsymbol{q} \frac{1}{q^2 - k_i^2 - \mathrm{i}\varepsilon} f_{\mathrm{UEBS}}(\boldsymbol{k}_f, 2\mathrm{s}, \boldsymbol{q}, 1\mathrm{s}) g_{\mathrm{B1}}^{(01)}(\boldsymbol{q}, 1\mathrm{s}, \boldsymbol{k}_i, 1\mathrm{s})$$
$$+(2\pi^2)^{-1} \int \mathrm{d}\boldsymbol{q} \frac{1}{q^2 - k_f^2 - \mathrm{i}\varepsilon} f_{\mathrm{UEBS}}(\boldsymbol{k}_f, 2\mathrm{s}, \boldsymbol{q}, 2\mathrm{s}) g_{\mathrm{B1}}^{(01)}(\boldsymbol{q}, 2\mathrm{s}, \boldsymbol{k}_i, 1\mathrm{s}) \qquad (2.33)$$

where $g_{\mathrm{B1}}^{(01)}(\boldsymbol{k}_f, n_f; \boldsymbol{k}_i, n_i)$ is the first Born exchange amplitude for the transition $(\boldsymbol{k}_i, n_i) \rightarrow (\boldsymbol{k}_f, n_f)$ from which the electron-nucleus interaction has been omitted. At large Δ, $g_{\mathrm{B1}}^{(01)}(\boldsymbol{k}_f, n\mathrm{s}; \boldsymbol{k}_i, n\mathrm{s})$ varies like $k_i^{-2}\Delta^{-4}$, and therefore the dominant contributions to g_{UEBS} arise from the first and last integrals in equation (2.33), which give contributions of order $k_i^{-3}\Delta^{-2}$, as in the elastic scattering case considered in I. However, since the direct scattering amplitude at large Δ is smaller for the 1s-2s transitions than for elastic scattering (by one inverse power of k_i) the *relative* importance of exchange is enhanced in the large-Δ limit, with respect to the elastic scattering case.

At small angles, the difference between the elastic and inelastic amplitudes is even more striking. Indeed, the term $g_{\mathrm{B1}}^{(01)}(\boldsymbol{k}_f, 1\mathrm{s}; \boldsymbol{k}_i, 1\mathrm{s})$ is of order k_i^{-2} at small angles and dominates the elastic exchange amplitude in that region, while the term $g_{\mathrm{B1}}^{(01)}(\boldsymbol{k}_f, 2\mathrm{s}, \boldsymbol{k}_i, 1\mathrm{s})$ varies like Δ^2/k_i^2 for small angles, and thus is of order k_i^{-4} in this angular range. In fact, for the inelastic transition $(\boldsymbol{k}_i, 1\mathrm{s}) \rightarrow (\boldsymbol{k}_f, 2\mathrm{s})$, the integral term in equations (2.32) which sums up all higher-order terms in perturbation theory exhibits a k_i^{-3} dependence, since $g_{\mathrm{B1}}(\boldsymbol{k}_f, 2\mathrm{s}; \boldsymbol{q}, n)$ is of order k_i^{-2} for important values of the intermediate momentum transfer $\boldsymbol{\Delta}_f = \boldsymbol{k}_f - \boldsymbol{q}$ and $f(\boldsymbol{q}, n; \boldsymbol{k}_i, 1\mathrm{s})$ is of order unity for the corresponding values of $\boldsymbol{\Delta}_i = \boldsymbol{k}_i - \boldsymbol{q}$. Thus the inelastic exchange amplitude is dominated by terms higher than first order at small angles as well as large angles. Moreover, because the direct amplitude is of order unity in the small-angle region, the effect of exchange in the inelastic case is smaller than for elastic scattering at small angles. This is rather fortunate, since an infinite number of terms in the summation of equations (2.32) are required for an accurate evaluation of the k_i^{-3} contribution, and closure methods are very suspect when used for the evaluation of exchange amplitudes. The 'elastic' approximation of equation (2.33) is also unreliable in this region, since only two intermediate states (1s and 2s) are used. Thus the approximation of (2.33) would be inaccurate for the analysis of 1s-2s spin-flip transitions at small angles, but it is adequate for the present study, where the exchange amplitude is combined with the direct one to construct singlet and triplet amplitudes.

An equation similar to (2.33) can of course be written for the 1s–2p transition, and the general conclusions obtained for the 1s-2s case are still valid for the 1s-2p process. In particular, the exchange amplitude $g_{\mathrm{UEBS}}(\boldsymbol{k}_f, 2\mathrm{p}, \boldsymbol{k}_i, 1\mathrm{s})$ is much smaller in the small-angle region than the direct amplitude, while at large angles its importance is enhanced with respect to elastic scattering because of the rapid fall-off of the first Born direct amplitude.

3. Results and discussion

3.1. *Elastic scattering*

Using the direct amplitude of equation (2.6) and the exchange amplitude (3.38) of I, we have calculated new UEBS differential and total cross sections for $e^{\pm}$-H(1s) elastic collisions. The second Born term $\bar{f}_{B2}$ was evaluated in the manner described in Byron and Joachain (1981), and the modified Wallace amplitude $\tilde{f}_W$ was obtained by using the method described in I to calculate f_W. Our results for elastic electron–atomic-hydrogen scattering at 100 and 200 eV are given in table 2, where they are compared with the recent theoretical calculations of Byron and Joachain (1981), Bransden *et al* (1982) and McCarthy and Stelbovics (1983a), and with the experimental data of Williams (1975). The agreement with experiment is satisfactory, but not excellent, and this is the case for all the theoretical results displayed in table 2. In contrast, it should be noted that except in the forward direction, the agreement between the theoretical values themselves is much better. In particular, our present results are in excellent agreement with the third-order optical model calculations of Byron and Joachain (1981), which correspond to another way of unitarising the EBS amplitude. At energies $E \geqslant 200$ eV, our new UEBS results are nearly identical with the previous UEBS results reported in I.

It is also instructive to compare various direct (no-exchange) differential cross sections. This is done in table 3 at an incident energy of 100 eV, where we show the results obtained from the Glauber amplitude, the EBS amplitude, the Wallace amplitude

Table 2. Differential and total cross sections for the elastic scattering of e^- by H(1s), in atomic units. Powers of ten are denoted by a superscript. Exp: differential cross sections measured by Williams (1975) (two significant figures are given with the error in the last figures in parentheses), total elastic (integrated) cross sections obtained by de Heer *et al* (1977) from the Williams' results, total cross sections obtained by summing the above elastic total cross sections and the inelastic ones given by de Heer *et al* (1977). A, present results; B, third-order optical model (Byron and Joachain 1981); C, three-state close-coupling with second-order pseudostate potentials (Bransden *et al* 1982); D, three-channel coupled-channels optical theory (McCarthy and Stelbovics 1983a).

	100 eV					200 eV				
θ (deg)	Expt	A	B	C	D	Expt	A	B	C	D
0	—	8.2	8.5	4.9	5.8	—	5.6	5.7	2.9	3.7
10	—	2.4	2.6	1.9	1.9	—	1.1	1.1	9.8^{-1}	1.0
20	1.1 (1)	8.5^{-1}	9.0^{-1}	8.0^{-1}	8.6^{-1}	4.2^{-1} (4)	3.8^{-1}	3.9^{-1}	3.8^{-1}	4.0^{-1}
30	5.1^{-1} (5)	3.6^{-1}	3.8^{-1}	3.8^{-1}	4.2^{-1}	1.7^{-1} (2)	1.5^{-1}	1.5^{-1}	1.5^{-1}	1.5^{-1}
40	2.9^{-1} (3)	1.7^{-1}	1.8^{-1}	1.9^{-1}	2.0^{-1}	7.1^{-2} (7)	6.2^{-2}	6.2^{-2}	6.2^{-2}	6.7^{-2}
60	7.2^{-2} (7)	5.3^{-2}	5.4^{-2}	5.9^{-2}	6.3^{-2}	1.9^{-2} (2)	1.6^{-2}	1.6^{-2}	1.7^{-2}	1.7^{-2}
80	3.0^{-2} (3)	2.3^{-2}	2.3^{-2}	2.4^{-2}	2.6^{-2}	8.6^{-3} (9)	6.4^{-3}	6.3^{-3}	6.5^{-3}	6.7^{-3}
100	1.6^{-2} (1)	1.2^{-2}	1.2^{-2}	1.3^{-2}	1.3^{-2}	4.1^{-3} (4)	3.2^{-3}	3.2^{-3}	3.3^{-3}	3.3^{-3}
120	9.2^{-3} (9)	8.0^{-3}	7.5^{-3}	8.2^{-3}	8.0^{-3}	2.7^{-3} (4)	2.0^{-3}	2.0^{-3}	2.0^{-3}	2.1^{-3}
140	6.5^{-3} (7)	5.9^{-3}	5.5^{-3}	6.0^{-3}	5.8^{-3}	1.8^{-3} (3)	1.4^{-3}	1.4^{-3}	1.4^{-3}	1.5^{-3}
160	—	5.0^{-3}	4.6^{-3}	5.0^{-3}	4.8^{-3}	—	1.2^{-3}	1.2^{-3}	1.2^{-3}	1.2^{-3}
180	—	4.7^{-3}	4.3^{-3}	4.8^{-3}	4.5^{-3}	—	1.1^{-3}	1.1^{-3}	1.2^{-3}	1.1^{-3}
σ_{el}	1.85	1.46	1.54	1.45	1.46	6.41^{-1}	6.17^{-1}	6.31^{-1}	5.8^{-1}	6.08^{-1}
σ_{tot}	6.85	7.04	7.68	8.03	6.49	4.18	4.23	4.38	3.7	3.9

Table 3. Differential cross sections (in $a_0^2\,sr^{-1}$) for elastic electron-atomic-hydrogen scattering, at an incident energy of 100 eV, calculated without the exchange contribution, as obtained from the Glauber (G), EBS (see equation (3.22) of I), many-body Wallace (W, see equation (3) of Byron *et al* 1981), previous UEBS (UEBS1, see equation (2.5)), modified many-body Wallace $\tilde{W}$, see equation (2.7)), present UEBS (UEBS2, see equation (2.6)) and third-order optical model (OM, see table 2 of Byron and Joachain 1981) approximations. Powers of ten are denoted by a superscript.

θ (deg)	G	EBS	W	UEBS1	$\tilde{W}$	UEBS2	OM
0	∞	8.01	∞	7.56	∞	7.49	7.89
5	2.54	4.31	2.94	4.00	2.87	3.94	4.27
10	1.35	2.27	1.66	2.08	1.62	2.05	2.25
20	5.46^{-1}	7.69^{-1}	7.14^{-1}	7.03^{-1}	7.09^{-1}	6.99^{-1}	7.61^{-1}
30	2.52^{-1}	3.20^{-1}	3.32^{-1}	2.92^{-1}	3.37^{-1}	2.98^{-1}	3.18^{-1}
40	1.25^{-1}	1.55^{-1}	1.63^{-1}	1.39^{-1}	1.70^{-1}	1.46^{-1}	1.54^{-1}
60	3.89^{-2}	5.08^{-2}	4.87^{-2}	4.34^{-2}	5.35^{-2}	4.82^{-2}	4.98^{-2}
80	1.63^{-2}	2.32^{-2}	1.95^{-2}	1.82^{-2}	2.26^{-2}	2.13^{-2}	2.17^{-2}
100	8.57^{-3}	1.33^{-2}	9.94^{-3}	9.53^{-3}	1.20^{-2}	1.16^{-2}	1.18^{-2}
120	5.41^{-3}	9.06^{-3}	6.12^{-3}	5.94^{-3}	7.62^{-3}	7.46^{-3}	7.55^{-3}
140	3.97^{-3}	7.02^{-3}	4.41^{-3}	4.31^{-3}	5.61^{-2}	5.53^{-3}	5.59^{-3}
160	3.32^{-3}	6.07^{-3}	3.66^{-3}	3.57^{-3}	4.71^{-2}	4.65^{-3}	4.70^{-3}
180	3.13^{-3}	5.79^{-3}	3.44^{-3}	3.36^{-3}	4.44^{-2}	4.39^{-3}	4.44^{-3}

f_W, the modified Wallace amplitude $\tilde{f}_W$, the UEBS direct amplitude f_{UEBS} of equation (2.5), the new UEBS amplitude $\tilde{f}_{UEBS}$ of equation (2.6) and the third-order optical model amplitude of Byron and Joachain (1981). Of particular interest is the fact that the modified Wallace amplitude $\tilde{f}_W$ leads to higher values of the differential cross section at intermediate and large angles than those obtained from f_W, with the consequence that the new UEBS values are in closer agreement with experiment than the ones presented in I. It is worth noting that the differences between the results using the Wallace amplitude f_W and those obtained from $\tilde{f}_W$ arise from fourth- and higher-order terms; these differences are seen to be substantial at large angles at 100 eV. As expected, they decrease with increasing energy, being negligible at an incident energy of 400 eV.

Turning now to positron impact, we present our new UEBS results for elastic differential cross sections, at 100 and 200 eV (at energies $E \geqslant 300$ eV, the new UEBS results are identical with the previous UEBS ones) in table 4, our total (integrated) elastic cross sections in table 5 and our total cross sections in table 6.

3.2. *The 1s–2s excitation process*

Our new UEBS results for 1s–2s excitation by electron impact have been calculated by using equation (2.6) for the direct amplitude, together with equation (2.33) for the exchange amplitude. The second Born term $\bar{f}_{B2}$ was evaluated by using the closure method with an average excitation energy $\bar{w} = 0.54$ au, and including the contributions from the 1s, 2s and 2p states exactly. At small angles the contributions from all the other p states have also been included exactly. The differential and total (integrated) cross sections obtained in this way are given in table 7 for incident energies of 100, 200, 300 and 400 eV, and compared with the theoretical results of Bransden *et al* (1982), McCarthy and Stelbovics (1983a), Kingston *et al* (1976) and Kingston and Walters (1980). At 100 and 200 eV, our results are in best agreement with those of Bransden *et al* (1982), except at intermediate angles, where our values lie between those obtained by Bransden *et al* and the three-state close-coupling calculations of Kingston *et al* (1976). The agreement between our calculations and the distorted-wave second Born results of Kingston and Walters (1980) is also quite good, becoming better as the energy increases. The main discrepancy is at intermediate angles, where the values of

Table 4. Differential cross sections for the elastic scattering of e^+ by H(1s), in units of $a_0^2\ sr^{-1}$. Powers of ten are denoted by a superscript. A, present results; B, third-order optical model (Byron and Joachain 1981).

	100 eV		200 eV	
θ (deg)	A	B	A	B
0	2.3	2.2	1.6	1.6
10	9.8^{-1}	9.7^{-1}	7.1^{-1}	7.0^{-1}
20	4.2^{-1}	4.1^{-1}	2.8^{-1}	2.8^{-1}
30	2.0^{-1}	2.0^{-1}	1.1^{-1}	1.1^{-1}
40	9.8^{-2}	1.0^{-1}	4.5^{-2}	4.6^{-2}
60	2.8^{-2}	3.1^{-2}	1.2^{-2}	1.2^{-2}
80	1.1^{-2}	1.3^{-2}	4.5^{-3}	4.7^{-3}
100	5.8^{-3}	6.9^{-3}	2.3^{-3}	2.4^{-3}
120	3.6^{-3}	4.3^{-3}	1.4^{-3}	1.5^{-3}
140	2.6^{-3}	3.2^{-3}	1.0^{-3}	1.1^{-3}
160	2.2^{-3}	2.7^{-3}	8.6^{-4}	9.0^{-4}
180	2.1^{-3}	2.5^{-3}	8.1^{-4}	8.5^{-4}

Table 5. Total elastic cross sections (in units of a_0^2) for positron scattering by atomic hydrogen.

Energy (eV)	First Born approximation	EBS†	Third-order optical model‡	Previous UEBS†	Present results (UEBS)
100	9.39^{-1}	7.59^{-1}	7.02^{-1}	7.15^{-1}	6.90^{-1}
200	4.84^{-1}	4.22^{-1}	4.13^{-1}	4.12^{-1}	4.12^{-1}
300	3.26^{-1}	2.95^{-1}	2.92^{-1}	2.91^{-1}	2.92^{-1}
400	2.46^{-1}	2.27^{-1}	2.26^{-1}	2.26^{-1}	2.26^{-1}

† Byron *et al* (1982).
‡ Byron and Joachain (1981).

Table 6. Total cross sections (units of a_0^2) for positron scattering by atomic hydrogen.

Energy (eV)	EBS†	Third-order optical model‡	Previous UEBS†	Present results (UEBS)
100	7.49	6.76	7.01	6.84
200	4.39	4.14	4.21	4.18
300	3.17	3.03	3.07	3.07
400	2.50	2.42	2.44	2.44

† Byron *et al* (1982).
‡ Byron and Joachain (1981).

Table 7. Differential and total cross sections for the excitation of the 2s state, in atomic units. Powers of ten are denoted by a superscript. A, present results; B, three-state close coupling with second-order pseudostate potentials (Bransden *et al* 1982); C, three-channel coupled-channels optical theory (McCarthy and Stelbovics 1983a); D, three-state close coupling (Kingston *et al* 1976); E, distorted-wave second Born approximation (Kingston and Walters 1980).

	100 eV					200 eV					300 eV			400 eV	
θ (deg)	A	B	C	D	E	A	B	C	D	E	A	D	E	A	E
0	1.1	9.3^{-1}	3.5	3.6	1.5	1.2	1.2	3.0	3.3	1.3	1.2	3.5	1.2	1.1	1.2
10	3.3^{-1}	3.0^{-1}	3.2^{-1}	3.7^{-1}	3.7^{-1}	2.5^{-1}	2.5^{-1}	2.4^{-1}	2.6^{-1}	2.7^{-1}	1.7^{-1}	1.8^{-1}	1.7^{-1}	1.1^{-1}	1.2^{-1}
20	6.6^{-2}	6.8^{-2}	7.3^{-2}	8.8^{-2}	7.5^{-2}	2.0^{-2}	2.3^{-2}	2.6^{-2}	2.8^{-2}	2.0^{-2}	7.6^{-3}	1.0^{-2}	7.2^{-3}	3.4^{-3}	3.2^{-3}
30	1.3^{-2}	1.1^{-2}	1.6^{-2}	2.0^{-2}	1.0^{-2}	3.2^{-3}	2.8^{-3}	3.9^{-3}	4.2^{-3}	2.6^{-3}	1.2^{-3}	1.5^{-3}	1.1^{-3}	5.6^{-4}	5.3^{-4}
40	5.7^{-3}	3.4^{-3}	6.4^{-3}	7.6^{-3}	3.8^{-3}	1.3^{-3}	1.2^{-3}	1.4^{-3}	1.6^{-3}	1.1^{-3}	4.5^{-4}	5.2^{-4}	4.3^{-4}	2.0^{-4}	2.0^{-4}
60	2.1^{-3}	1.6^{-3}	2.5^{-3}	2.7^{-3}	2.0^{-3}	3.4^{-4}	2.9^{-4}	3.9^{-4}	4.1^{-4}	3.4^{-4}	1.1^{-4}	1.3^{-4}	1.1^{-4}	4.6^{-5}	4.8^{-5}
80	8.6^{-4}	7.6^{-4}	1.1^{-3}	1.3^{-3}		1.2^{-4}	1.3^{-4}	1.5^{-4}	1.6^{-4}		3.8^{-5}	4.7^{-5}		1.7^{-5}	
100	4.3^{-4}	4.2^{-4}	6.1^{-4}	7.1^{-4}		6.0^{-5}	5.6^{-5}	7.8^{-5}	8.0^{-5}		1.9^{-5}	2.3^{-5}		8.1^{-6}	
120	2.6^{-4}	2.8^{-4}	3.9^{-4}	4.7^{-4}	2.9^{-4}	3.6^{-5}	4.1^{-5}	4.6^{-5}	5.1^{-5}	3.9^{-5}	1.1^{-5}	1.4^{-5}	1.2^{-5}	5.0^{-6}	4.7^{-6}
140	1.9^{-4}	2.2^{-4}	3.0^{-4}	3.6^{-4}	2.2^{-4}	2.6^{-5}	2.7^{-5}	3.5^{-5}	3.8^{-5}	2.8^{-5}	8.0^{-6}	9.8^{-6}	8.7^{-6}	3.5^{-6}	3.4^{-6}
160	1.6^{-4}	1.9^{-4}	2.4^{-4}	3.1^{-4}	1.8^{-4}	2.1^{-5}	2.5^{-5}	3.1^{-5}	3.3^{-5}	2.3^{-5}	6.6^{-6}	7.7^{-6}	7.2^{-6}	2.9^{-6}	2.7^{-6}
180	1.5^{-4}	1.6^{-4}	2.3^{-4}	3.0^{-4}	1.7^{-4}	2.0^{-5}	2.1^{-5}	2.7^{-5}	3.2^{-5}	2.2^{-5}	6.1^{-6}			2.7^{-6}	
σ_{2s}	1.2^{-1}	1.1^{-1}	1.6^{-1}	1.8^{-1}	1.3^{-1}	7.6^{-2}	7.5^{-2}	9.1^{-2}	9.4^{-2}	9.3^{-2}	6.2^{-2}	6.3^{-2}	6.2^{-2}	4.3^{-2}	4.7^{-2}

Kingston and Walters are lower than ours. It is worth pointing out that in contrast with several other calculations our results do not exhibit any shoulder at intermediate angles.

The only measurements available at intermediate energies are those of Williams (1981), performed at an energy of 54.4 eV (corresponding to the value $k_i = 2$). In figure 1, we compare our new UEBS calculations with these measurements, and also show the influence of exchange effects. The agreement with the data is fair in view of the fact that $k_i = 2$ may be considered as a lower limit for the applicability of our method.

In table 8 we compare the differential cross sections obtained from various theoretical methods, with exchange omitted. It is seen that, as for elastic scattering (see table 3), the values calculated using $\tilde{f}_W$ are higher than those obtained from f_W at large angles, with the consequence that the new UEBS values are higher than the previous ones in this angular region. Nevertheless, the differences between the two sets of UEBS results is relatively small. The main differences between the 1s–2s cross sections of this paper and those we obtained previously (Byron *et al* 1981) comes from the treatment of the exchange amplitude, the second-order approximation of Byron *et al* (1981) being replaced by the non-perturbative calculation based on equation (2.33).

3.3. *The 1s–2p excitation process*

We have obtained our results for 1s–2p excitation by electron impact by using equation (2.6) for the direct amplitude. The second Born term $\bar{f}_{B2}$ was evaluated by using the

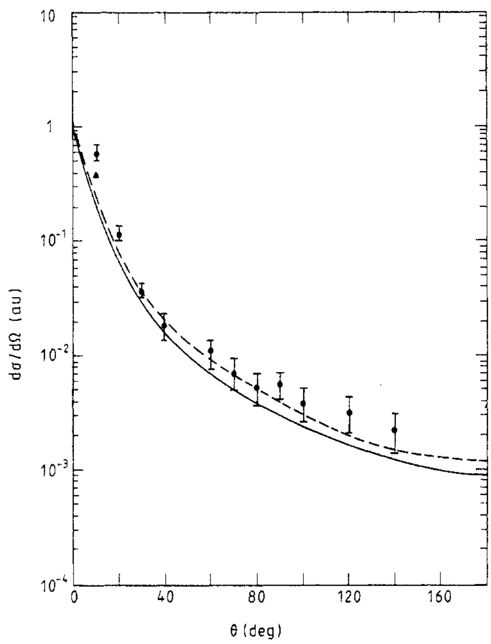

Figure 1. The excitation of atomic hydrogen to the 2s state by electron impact at 54.4 eV. ——, present UEBS results; -----, present UEBS results without exchange. The ▲ and ● represent the experimental data of Williams (1981), obtained from the ratio $\sigma(2s)/\sigma(2p)$ (▲) or from the sum $\sigma(2s)+\sigma(2p)$ (●).

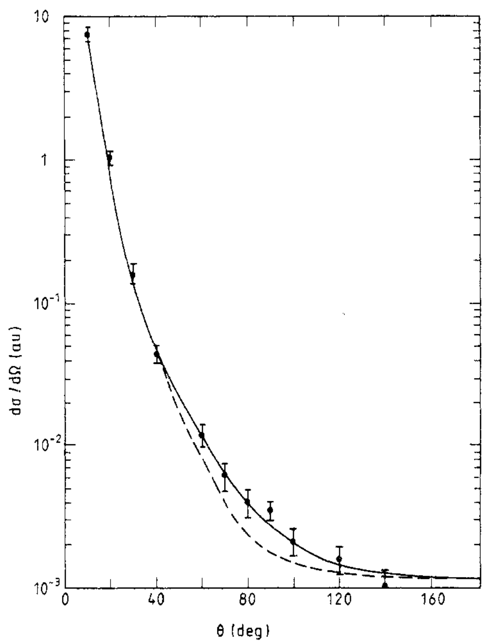

Figure 2. The excitation of atomic hydrogen to the 2p state by electron impact at 54.4 eV. ——, present UEBS results; -----, present UEBS results without exchange. ●, experimental data of Williams (1981).

Table 8. Differential cross section (in $a_0^2\,\mathrm{sr}^{-1}$) for excitation of the 2s state of atomic hydrogen by electron impact, calculated without exchange, as obtained from Glauber (G), Wallace (W, see equation (3) of Byron *et al* 1981), previous UEBS (UEBS1, equation (2.5)), modified Wallace ($\tilde{W}$, equation (2.7)) and present UEBS (UEBS2, equation (2.6)) approximations. The incident energy is 100 eV. Powers of ten are denoted by a superscript.

θ (deg)	G	W	UEBS1	$\tilde{W}$	UEBS2
0	1.90	2.01	1.15	2.01	1.15
10	4.38^{-1}	4.81^{-1}	3.35^{-1}	4.81^{-1}	3.35^{-1}
20	7.43^{-2}	7.58^{-2}	7.14^{-2}	7.79^{-2}	7.35^{-2}
30	1.31^{-2}	1.24^{-2}	1.50^{-2}	1.37^{-2}	1.64^{-2}
40	4.51^{-3}	4.76^{-3}	5.93^{-3}	5.50^{-3}	6.77^{-3}
60	1.62^{-3}	1.86^{-3}	2.05^{-3}	2.19^{-3}	2.42^{-3}
80	7.45^{-4}	8.21^{-4}	8.69^{-4}	9.97^{-4}	1.06^{-3}
100	4.05^{-4}	4.24^{-4}	4.41^{-4}	5.33^{-4}	5.58^{-4}
120	2.57^{-4}	2.60^{-4}	2.67^{-4}	3.35^{-4}	3.48^{-4}
140	1.89^{-4}	1.86^{-4}	1.91^{-4}	2.44^{-4}	2.52^{-4}
160	1.58^{-4}	1.53^{-4}	1.56^{-4}	2.03^{-4}	2.10^{-4}
180	1.49^{-4}	1.43^{-4}	1.45^{-4}	1.91^{-4}	1.97^{-4}

closure method with an average excitation energy $\bar{w} = 0.54$ au, and including the 1s, 2s and 2p states exactly. Due to major computational difficulties, we were unable to calculate the exchange amplitude from an equation analogous to equation (2.33), which was used for the 1s–2s transition. Instead, we used the first-order amplitude $g_{\mathrm{B1}}^{(01)}$, i.e. the first Born exchange term from which the electron-nucleus interaction has been removed. Our calculated differential and total (integrated) cross sections are given in table 9 for incident energies ranging from 100 to 400 eV; they are compared with the theoretical results of Bransden *et al* (1983), McCarthy and Stelbovics (1983a), Kingston *et al* (1976) and Kingston and Walters (1980). The comments made above concerning the comparison of the various theoretical results for the 1s–2s transition also apply in this case.

In figure 2 we compare our UEBS results at an energy of 54.4 eV with the differential cross sections measured by Williams (1981). The agreement is seen to be excellent. Also shown for comparison are the results of our calculations without exchange.

In figure 3 we compare, at an incident energy of 100 eV, the direct (no-exchange) differential cross sections obtained from different eikonal approximations. Two important features emerge from this figure. The first one is the failure of the Glauber approximation for s–p transitions at large angles, which is corrected by the Wallace amplitudes f_{W} and $\bar{f}_{\mathrm{W}}$; this is mainly due to the non-Glauber second-order term Re $\bar{f}_{\mathrm{W2}}$ which is present in the Wallace amplitudes. The second one is the fact that the 'edge' structure near $\theta = 30°$ (not seen experimentally at 54.4 eV), present in the Wallace approximation, disappears in the UEBS method. Finally, we remark that in contrast to the results obtained by Unnikrishnan and Prasad (1982), we do not observe any steady increase of our Wallace differential cross sections at large angles. We note in this connection that the differentiations required to obtain our Wallace amplitudes were all done analytically using the algebraic programming system REDUCE; this procedure is very useful in avoiding loss of precision.

Let us now turn to a more detailed study of the 1s–2p excitation process using a coordinate system in which the Z axis (the quantisation axis for the 2p states) lies along the incident momentum $\boldsymbol{k}_i$. In figure 4, we show the differential cross section

Table 9. Differential and total cross sections for the excitation of the 2p state, in atomic units. Powers of ten are denoted by a superscript. A, present results; B, three-state close coupling with second-order pseudostate potentials (Bransden *et al* 1982); C, three-channel coupled-channels optical theory (McCarthy and Stelbovics 1983a); D, three-state close coupling (Kingston *et al* 1976); E, distorted-wave second Born approximation (Kingston and Walters 1980).

	100 eV					200 eV					300 eV			400 eV	
θ (deg)	A	B	C	D	E	A	B	C	D	E	A	D	E	A	E
0	9.2^{+1}	9.7^{+1}	8.8^{+1}	8.9^{+1}	9.9^{+1}	2.1^{+2}	2.5^{+2}	2.0^{+2}	2.0^{+2}	2.1^{+2}	3.3^{+2}	3.2^{+2}	3.3^{+2}	4.4^{+2}	4.5^{+2}
10	3.9	4.2	4.4	4.6	4.6	1.3	1.5	1.5	1.6	1.5	5.8^{-1}	6.7^{-1}	6.3^{-1}	2.8^{-1}	3.0^{-1}
20	2.1^{-1}	2.1^{-1}	3.0^{-1}	3.2^{-1}	2.3^{-1}	2.8^{-2}	2.4^{-2}	3.6^{-2}	3.8^{-2}	2.6^{-2}	6.5^{-3}	7.8^{-3}	5.4^{-3}	2.1^{-3}	1.7^{-3}
30	2.3^{-2}	1.2^{-2}	2.8^{-2}	3.0^{-2}	1.4^{-2}	2.2^{-3}	1.6^{-3}	2.1^{-3}	2.4^{-3}	1.6^{-3}	5.7^{-4}	5.6^{-4}	4.8^{-4}	2.2^{-4}	2.0^{-4}
40	6.4^{-3}	3.0^{-3}	6.8^{-3}	6.4^{-3}	4.1^{-3}	6.7^{-4}	5.2^{-4}	6.7^{-4}	6.7^{-4}	6.0^{-4}	1.9^{-4}	1.9^{-4}	1.8^{-4}	7.7^{-5}	7.6^{-5}
60	1.4^{-3}	1.4^{-3}	1.7^{-3}	1.5^{-3}	1.4^{-3}	1.8^{-4}	2.0^{-4}	1.9^{-4}	1.9^{-4}	2.0^{-4}	5.6^{-5}	6.1^{-5}	5.8^{-5}	2.4^{-5}	2.4^{-5}
80	6.2^{-4}	6.3^{-4}	6.8^{-4}	7.4^{-4}		9.3^{-5}	1.1^{-4}	9.3^{-5}	9.5^{-5}		3.0^{-5}	3.0^{-5}		1.3^{-5}	
100	4.2^{-4}	3.9^{-4}	4.1^{-4}	4.7^{-4}		6.4^{-5}	6.6^{-5}	6.3^{-5}	6.4^{-5}		2.0^{-5}	2.1^{-5}		8.8^{-6}	
120	3.4^{-4}	2.8^{-4}	2.8^{-4}	3.5^{-4}	3.9^{-4}	5.0^{-5}	6.0^{-5}	4.6^{-5}	4.8^{-5}	5.1^{-5}	1.6^{-5}	1.4^{-5}	1.6^{-5}	6.8^{-6}	6.9^{-6}
140	3.0^{-4}	2.5^{-4}	2.2^{-4}	2.8^{-4}	3.8^{-4}	4.3^{-5}	4.7^{-5}	3.9^{-5}	4.1^{-5}	4.2^{-5}	1.3^{-5}	1.2^{-5}	1.4^{-5}	5.8^{-6}	5.7^{-6}
160	2.8^{-4}	2.1^{-4}	1.9^{-4}	2.4^{-4}	3.7^{-4}	3.9^{-5}	5.1^{-5}	3.4^{-5}	3.7^{-5}	3.5^{-5}	1.2^{-5}	9.0^{-6}	1.3^{-5}	5.3^{-6}	5.1^{-6}
180	2.7^{-4}	2.3^{-4}	1.8^{-4}	2.3^{-4}		3.8^{-5}	3.1^{-5}	3.1^{-5}	3.3^{-5}		1.2^{-5}			5.1^{-6}	
σ_{2p}	1.9	2.1	2.1	2.1	2.2	1.3	1.6	1.4	1.4	1.5	9.5^{-1}	1.1	1.1	8.2^{-1}	9.0^{-1}

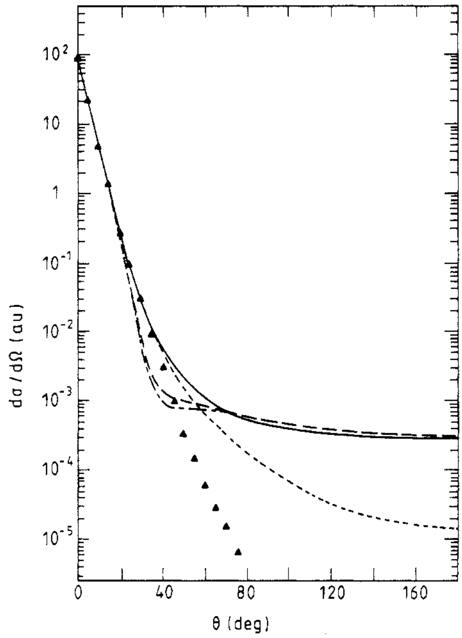

Figure 3. The excitation of atomic hydrogen to the 2p state by electron impact at 100 eV, without exchange. ——, present UEBS results; -----, Glauber approximation; – – – –, Wallace approximation (see equation (3) of Byron *et al* 1981); - - -, modified Wallace approximation (equation (2.7)); ▲, first Born approximation.

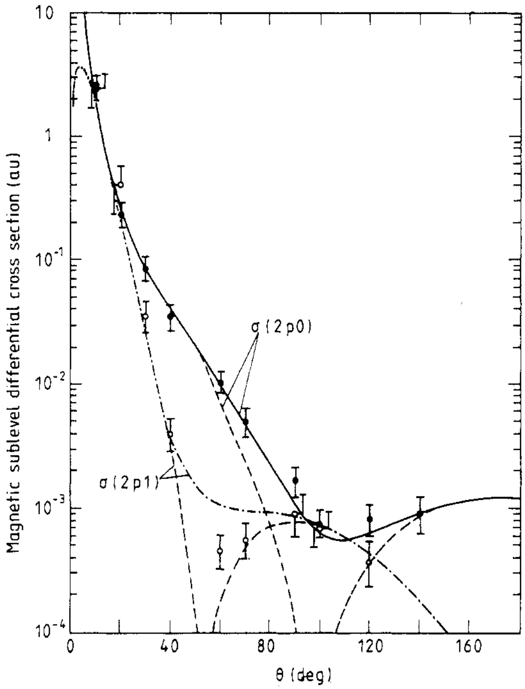

Figure 4. Magnetic sublevel differential cross section for the excitation of atomic hydrogen to the 2pm states by electron impact at 54.4 eV. ——, present UEBS results for the excitation of the 2p0 state; — · —, present UEBS results for the excitation of the 2p1 (or 2p−1) state; -----, present UEBS results without exchange; ●, experimental data of Williams (1981) for the excitation of the 2p0 state; ○, experimental data of Williams (1981) for the excitation of the 2p1 (or 2p−1) state.

for excitation of the magnetic sublevels $m=0$ and $m=\pm 1$ by electron impact, at an incident energy of 54.4 eV. Our UEBS results are compared with the experimental data of Williams (1981). The agreement is seen to be excellent for the $m=0$ excitation over the entire angular region; it is also very good for the $m=\pm 1$ excitation process, except for scattering angles between 50 and 80°. It should be noted that the $m=\pm 1$ differential cross section is very sensitive to exchange effects in this angular range; this is also the case for the $m=0$ differential cross section in the vicinity of $\theta=100°$.

The angular correlation parameters λ, R and I (see for example Slevin 1984) are defined by

$$\lambda=\frac{\sigma_0}{\sigma}=\frac{\sigma_0}{\sigma_0+2\sigma_1} \tag{3.1a}$$

$$R=\frac{\operatorname{Re}\langle a_0 a_1^*\rangle}{\sigma} \tag{3.1b}$$

$$I=\frac{\operatorname{Im}\langle a_0 a_1^*\rangle}{\sigma} \tag{3.1c}$$

where σ_0 and σ_1 are respectively the differential cross sections for the excitation of the 2p0 and 2p1 states, $\sigma = \sigma_0 + 2\sigma_1$, a_0 and a_1 are respectively the amplitudes for the excitation of these states (with the factor $\exp(im\phi_\Delta)$ removed) and $\langle\ \rangle$ denotes the statistical average of the singlet and triplet amplitudes. The parameters λ, R and I are shown in figure 5 for an incident electron energy of 54.4 eV. Our values for the parameter λ are seen to be in good agreement with the experimental results of Weigold

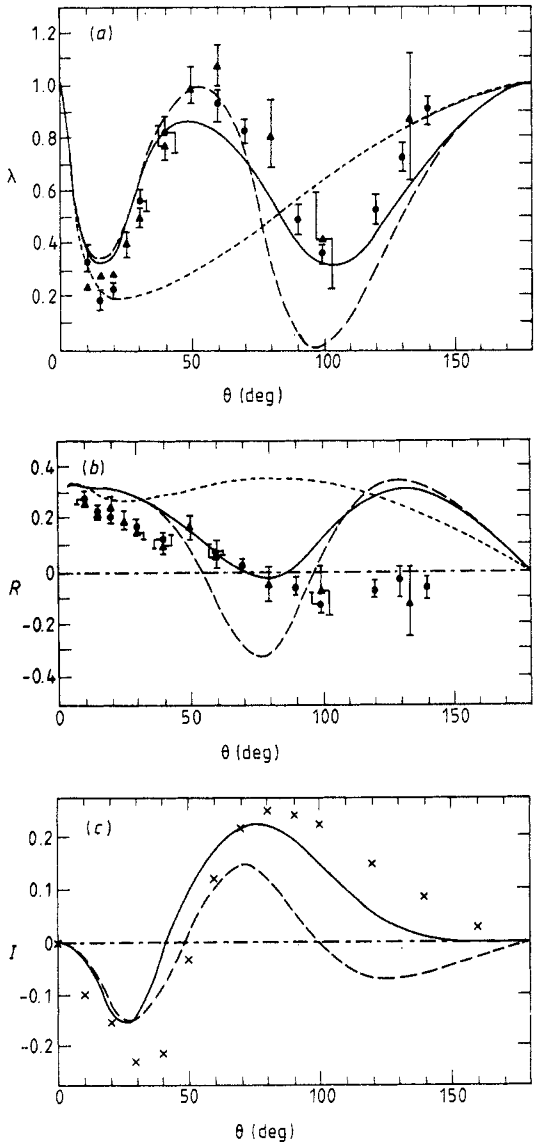

Figure 5. Variation of (a) λ, (b) R and (c) I with the electron scattering angle for an incident energy of 54.4 eV. ——, present UEBS results; — —, present UEBS results without exchange; ×, three-state close coupling (Kingston *et al* 1982); -----, 'geometrical' values given by equations (3.2). Experimental results; ▲, Weigold *et al* (1980); ●, Williams (1981).

et al (1980) and Williams (1981) over the entire angular region. This is not the case with the parameter R, where there is a marked disagreement between our calculated values and experiment at large angles. It is important to emphasise that this disagreement is present in all recent theoretical calculations (see for example Bransden *et al* 1982, Edmunds *et al* 1983, Fargher and Roberts 1983, Kingston *et al* 1982, Morgan 1982, McCarthy and Stelbovics 1983a, b, Madison 1984). It is worth noting that our results for both parameters λ and R are in excellent agreement with the recent full second-order distorted-wave calculation carried out by Madison (1984). For the parameter I, no experimental results are available yet. It is seen that our theoretical values are in qualitative agreement with the three-state close-coupling calculations of

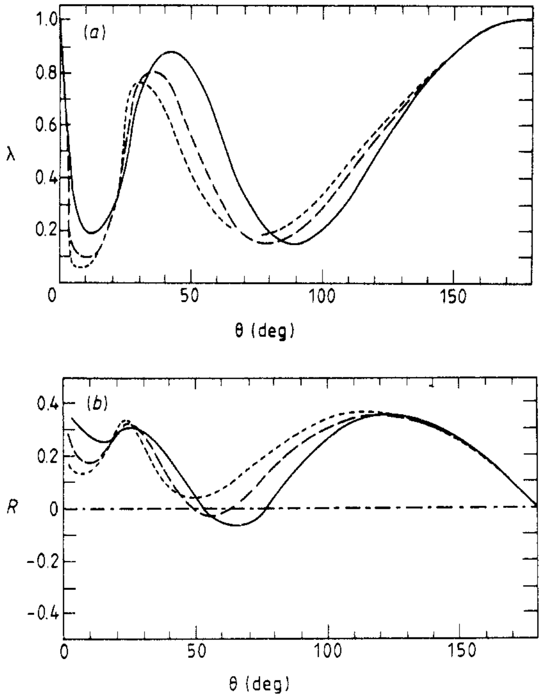

Figure 6. Variation of (a) λ and (b) R with electron scattering angle and incident energy in the present UEBS approximation. ——, 100 eV, — —, 200 eV, ----- 400 eV.

Table 10. The angular correlation parameters λ and R at 100 eV. A, present results; B, three-state close coupling with second-order pseudostate potentials (Bransden *et al* 1982); E1, experimental results of Hood *et al* (1979); E2, experimental results of Slevin *et al* (1980).

	λ				R			
θ (deg)	A	B	E1	E2	A	B	E1	E2
3	—	—	—	0.39	—	—	—	0.23
5	0.32	0.30	—	0.09	0.33	0.32	—	0.19
10	0.17	0.14	0.194	0.02	0.26	0.25	0.175	0.15
15	0.18	0.13	0.183	0.18	0.25	0.23	0.148	0.11

Kingston *et al* (1982). As in figure 4, the influence of exchange effects is important at intermediate angles; this is in contrast with the conclusions reached by Morgan (1982), who performed close-coupling calculations for this process and found that the parameters λ and R were rather insensitive to exchange effects.

We display in figure 6 our λ and R parameters at 100, 200 and 400 eV to show the trends of these quantities with increasing energy. A detailed comparison of our values

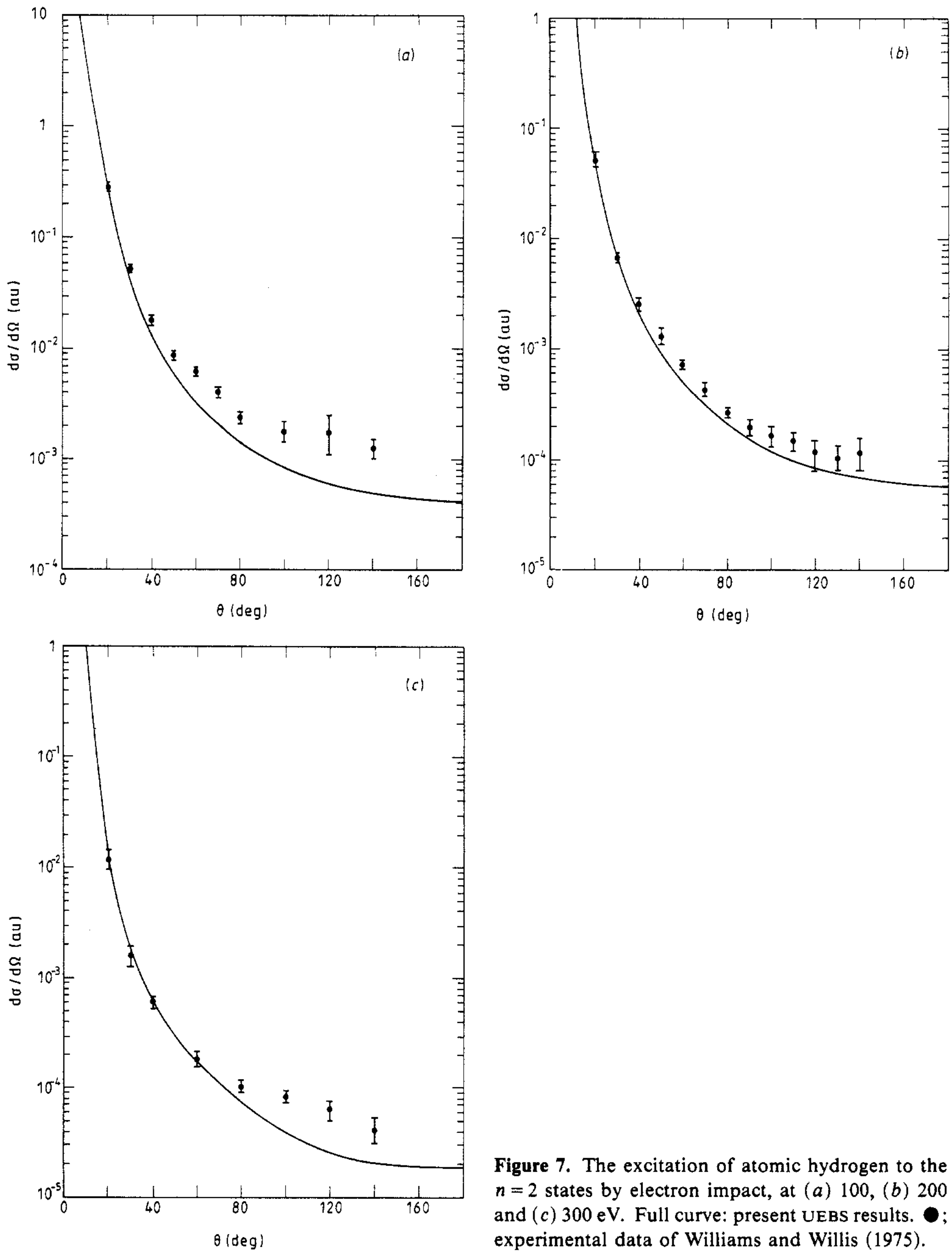

Figure 7. The excitation of atomic hydrogen to the $n = 2$ states by electron impact, at (*a*) 100, (*b*) 200 and (*c*) 300 eV. Full curve: present UEBS results. ●; experimental data of Williams and Willis (1975).

for λ and R with those calculated by Bransden *et al* (1982) and with the experimental values of Hood *et al* (1979) and Slevin *et al* (1980) is given in table 10 at 100 eV, for small scattering angles $\theta \leqslant 15°$. At 350 eV, there are recent measurements of λ and R parameters at small angles by Back *et al* (1984); our corresponding UEBS results in this angular region are very close to the distorted-wave second Born values of Walters (quoted by Back *et al* 1984), in disagreement with the experimental values.

We also show in figures 5(a) and 5(b) the purely 'geometrical' values

$$\lambda = \cos^2 \theta_\Delta \tag{3.2a}$$

$$R = -\sin \theta_\Delta \cos \theta_\Delta/\sqrt{2} \tag{3.2b}$$

which are obtained in the first Born, Glauber and Wallace approximations (θ_Δ is the angle between the momentum transfer and the direction of the incident particle). Moreover, the parameter $I \equiv 0$ in these three approximations. Clearly a proper treatment of second-order effects via the second Born term is necessary in order to obtain meaningful results for the correlation parameters.

3.4. *The* $n = 1 \rightarrow n = 2$ *transition*

Finally, we show in figure 7(a), (b) and (c) our UEBS values for the sum of the 1s-2s and 1s-2p differential cross sections, at energies of 100, 200 and 300 eV, they are compared with the experimental data of Williams and Willis (1975). The agreement at small angles is very good, but at large angles it is seen to deteriorate. Our results being in good agreement with those of Kingston and Walters (1980) and both theoretical calculations being on very firm theoretical ground at an incident energy of 300 eV, it is unlikely that the origin of the discrepancy is due to the theory.

References

Back C G, Watkin S, Eminyan M, Rubin K, Slevin J and Woolsey J M 1984 *J. Phys. B: At. Mol. Phys.* **17** 2695-706
Bransden B H, Scott T, Shingal R and Raychoudhury R K 1982 *J. Phys. B: At. Mol. Phys.* **15** 4605-16
Burke P G and Williams J F 1977 *Phys. Rep.* **34** 325-69
Byron F W Jr and Joachain C J 1973 *Phys. Rev.* A **8** 3266-9
—— 1977 *Phys. Rep.* **34** 233-324
—— 1981 *J. Phys. B: At. Mol. Phys.* **14** 2429-48
Byron F W Jr, Joachain C J and Potvliege R M 1981 *J. Phys. B: At. Mol. Phys.* **14** L609-15
—— 1982 *J. Phys. B: At. Mol. Phys.* **15** 3915-43
Byron F W Jr and Latour L J 1976 *Phys. Rev.* A **13** 649-64
Edmunds P W, McDowell M R C and Morgan L A 1983 *J. Phys. B: At. Mol. Phys.* **16** 2553-66
Fargher H E and Roberts M J 1983 *J. Phys. B: At. Mol. Phys.* **16** 4427-36
Fon W C, Berrington K A, Burke P G and Kingston A E 1981 *J. Phys. B: At. Mol. Phys.* **14** 1041-51
de Heer F J, McDowell M R C and Wagenaar R W 1977 *J. Phys. B: At. Mol. Phys.* **10** 1945-53
Hood S T, Weigold E and Dixon A J 1979 *J. Phys. B: At. Mol. Phys.* **12** 631-45
Joachain C J 1983, *Quantum Collision Theory* 3rd ed (Amsterdam: North-Holland) ch 15
Kingston A E, Fon W C and Burke P G 1976 *J. Phys. B: At. Mol. Phys.* **9** 605-18
Kingston A E, Liew Y C and Burke P G 1982 *J. Phys. B: At. Mol. Phys.* **15** 2755-66
Kingston A E and Walters H R J 1980 *J. Phys. B: At. Mol. Phys.* **13** 4633-62
Madison D H 1984 *Phys. Rev. Lett.* **53** 42-5
Morgan L A 1982 *J. Phys. B: At. Mol. Phys.* **15** 4247-57

McCarthy I E and Stelbovics A T 1983a *J. Phys. B: At. Mol. Phys.* **16** 1233–45
—— 1983b *J. Phys. B: At. Mol. Phys.* **16** 1611–7
—— 1983c *Phys. Rev.* A **28** 2693–707
Slevin J 1984 *Rep. Prog. Phys.* **47** 461–512
Slevin J, Eminyan M, Woolsey J M, Vassilev G and Porter H Q 1980 *J. Phys. B: At. Mol. Phys.* **13** L341–5
Unnikrishnan K and Prasad M A 1982 *J. Phys. B: At. Mol. Phys.* **15** 1549–57
Wallace S J 1973 *Ann. Phys., NY* **78** 190–257
Weigold E, Frost L and Nygaard K J 1980 *Phys. Rev.* A **21** 1950–4
Williams J F 1975 *J. Phys. B: At. Mol. Phys.* **8** 2191–9
—— 1981 *J. Phys. B: At. Mol. Phys.* **14** 1197–217
Williams J F and Willis B A 1975 *J. Phys. B: At. Mol. Phys.* **8** 1641–69